Collaborative Search and Pursuit for Autonomous Helicopters

Eric N. Johnson
eric.johnson@ae.gatech.edu
Lockheed Martin Associate Professor of Avionics Integration

John G. Mooney
john.g.mooney@gatech.edu
Graduate Research Assistant

Georgia Institute of Technology
Atlanta, Georgia

ABSTRACT

This paper describes recent results from the Georgia Institute of Technology to develop, improve, and flight test a multi-aircraft collaborative architecture, focused on decentralized autonomous decision-making. The architecture includes a search coverage algorithm, behavior estimation, and a pursuit algorithm designed to solve a scenario-driven challenge problem. The architecture was implemented on a pair of Yamaha RMAX helicopters outfitted with modular avionics, as well as an associated set of simulation tools. Simulation and flight test results for single- and multiple-aircraft scenarios are presented. Further work suggested includes identification and development of more sophisticated methods that can replace the simpler elements in modular fashion.

INTRODUCTION

As applications for military and civil unmanned aerial systems continue to grow, the ability to use a collaborating team of UAS will, in many cases, have an advantage over operating a single UAS. Owners/operators can invest in a number of simple, smaller, inexpensive aircraft, rather than a single aircraft. Teaming presents an increased degree of robustness, as the loss of a single aircraft no longer results in mission failure nor requires costly replacement. Moreover, the damage from a crash to people or property on the ground is reduced. By definition, a team of UASs is in multiple places at once, meaning a wider sensor net can be cast. Heterogeneous sensor packages, which can be tailored to the mission and environment, can be added to or removed from the team very easily.

However, there are costs associated with UAS collaboration. Establishing communication, task allocation, coordination, synchronization, collision avoidance, and an effective user interface are just the beginning of the problem. This paper focuses on use of one or two aircraft to collaborate to solve a scenario-driven challenge problem, focused on decentralized autonomous aircraft guidance.

Challenge Problem and Assumptions

The aircraft are given the mission to find a fugitive who has entered a small urban area, and drive him toward a designated capture location. We assume that the evader behaves in mostly predictable ways, following a general set of rules. First, the evader stays inside the designated area (as this area is a safe haven for him), but will not enter a building for fear of being immobilized there. We also assume that the evader moves strictly based on the relative position of the nearest search aircraft, and selects a locally constant evasion direction, subject to the above constraints. The evader will always have an accurate estimate of his own position, of aircraft positions, and of terrain in the search area. The aircraft can communicate with each other their own state and their estimates of the evader location and the terrain. They can detect the evader when he is in line of sight and within a specified range. He will occasionally select a new direction after an arbitrary amount of time. When the evader has been driven to the capture area, the problem is complete.

Review of Relevant Literature

Multi-robot coordination and information sharing has been studied by many researchers, primarily in the last 20 years. These efforts have investigated multiple paradigms of control and coordination. Arkin (Ref. 1), Balch (Ref. 2), and Parker (Ref. 3), for example, have focused on reactive behavior-based control and interaction. This approach assumes minimal or no direct communication between robots, often relying upon the robot's ability to observe the behavior of other robots to coordinate efforts. Other efforts have maintained decentralized control, but allowed robots to explicitly share state information (Ref. 4). Others use a fully-centralized approach, treating the system as a single meta-robot with a very high-dimension configuration space (Refs. 5, 6). Coordination of robotic aircraft has been studied extensively as well, though usually in the context of collision avoidance or formation control (Refs. 7–9). Previous work on autonomous collaborative search has demonstrated the effectiveness of spiral and lane-based search patterns using appropriate objective

Presented at the 70th AHS Annual Forum, Montreal, Quebec, Canada, May 20–22, 2014.

functions and heuristics (Refs. 10, 11). More recently, Mezic and Mathew, with other authors, have published a number of sophisticated techniques for centralized control of mobile sensors to provide uniform coverage of an area (Refs. 12–16). In this work they derived several algorithms through rigorous analysis, which they dubbed "Spectral Multiscale Coverage" and "Multiscale Adaptive Search", and tested their performance in simulation and flight test (Ref. 17). The work presented here builds upon that in (Ref. 18), adding the complexity of searching for a moving target as well as the estimation and pursuit of that target.

GENERAL APPROACH

Collaborative Search

The algorithm used for collaborative search in these experiments is designed to be simple, robust, and able to be executed effectively using de-centralized guidance. Additionally, the search strategy ideally would not result in predictable flight paths which would place the aircraft at risk and allow the evader to hide more effectively. The sensor package available includes both laser range-finding to characterize the terrain, and a notional sensor which can detect an evader in line-of-sight within a finite radius.

The general approach is to discretize the search area into reasonably sized pixels, which record the last time they had been observed. These pixels need to be large enough that the entire search area can be represented in a reasonable amount of memory, yet small enough that a single measurement in that pixel can effectively approximate the entire pixel.

Half the time, the aircraft then chooses a point in the map which reasonably balances the demands to observe areas which have not been recently observed and maintaining separation from each other (as measured by the cost function in Equation 1). To speed this process, the point is selected from a random sample of the search area. The other half of the time, the aircraft selects a point in the search area at random, discarding points which are too close to the other aircraft. Obstacle avoidance is accomplished using the simple scan algorithm detailed in (Ref. 19). Collision avoidance between the aircraft is accomplished by a simple set of heuristics.

$$
\begin{aligned}
J = &-\alpha_0(\text{time since last observation})^2 \\
&+\alpha_1\frac{(\text{distance to other aircraft})}{(\text{mapping speed})}
\end{aligned} \tag{1}
$$

Evader Simulation Model

Evader motion model designed to be relatively simple but have realistic-looking motion for a human being running and attempting to change direction. This is modeled by the evader have a maximum amount of power which can be applied to either running faster or changing directions. Equations 2 through 5 describe the equations of motion used.

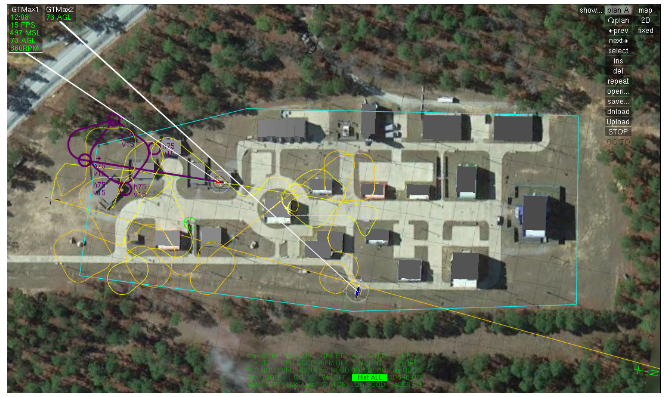

Fig. 1: Aircraft in collaborative search mode.

$$
\begin{Bmatrix} \dot{x}_E \\ \dot{y}_E \\ \dot{V} \\ \dot{\psi} \end{Bmatrix} = \begin{Bmatrix} V\cos(\psi) \\ V\sin(\psi) \\ -\frac{1}{\tau_V}V + \frac{1}{\tau_V}V_{cmd} \\ \dot{\psi}_{cmd} \end{Bmatrix} \tag{2}
$$

subject to

$$
P_{avail} = P_{max} - P_{max}\frac{V^3}{V_{max}^3} \tag{3}
$$

$$
V_{cmd} \leq V_{max} \tag{4}
$$

$$
\dot{\psi}_{cmd} \leq \dot{\psi}_{max}\frac{P_{avail}}{P_{max}} \tag{5}
$$

The evader's actions to follow the rules described above are modeled using the simple control logic below.

$$
V_{cmd} = V_{max}\left(1 - \frac{k(\psi_{cmd} - \psi)}{\dot{\psi}_{max}}\right) \tag{6}
$$

$$
\psi_{cmd} = \psi_{pursuer} + \psi_{evasion} \tag{7}
$$

$$
\psi_{pursuer} = \arctan\left(\frac{r_{P\to E}}{r_{P\to E}{}^T r_{P\to E}}\right) \tag{8}
$$

$$
r_{P\to E} = \begin{Bmatrix} x_P \\ y_P \end{Bmatrix} - \begin{Bmatrix} x_E \\ y_E \end{Bmatrix} \tag{9}
$$

and k, τ_V, V_{max}, and $\dot{\psi}_{max}$ are assumed to be constant, and subscripts P and E represent the nearest pursuer and evader, respectively.

The evader model also is subject to obstacle constraints, reducing its speed in the direction of an obstacle proportional to the distance from the obstacle. Finally, we assume that the evader treats the search area boundary as an obstacle.

Evader Estimation

The pursuit algorithm uses a significantly simpler model as the basis for a linear Kalman Filter (KF) to estimate evader location and velocity. The equations describing the KF are omitted here for brevity. This simplified model treats changes in velocity as a random process to be estimated through observation. The evasion strategy ("$\psi_{evasion}$") is estimated using a proportional first-order observer with constant gain, using the evader's estimated heading and bearing to the nearest aircraft as measurement updates (Equation 10). To reduce complexity, obstacle constraints are not considered.

$$\begin{aligned}\hat{\psi}_{evasion,k+1} &= \hat{\psi}_{evasion,k} \\ &+ \left(\hat{\psi} - \arctan(y_P - y_E, x_P - x_E) - \hat{\psi}_{evasion,k}\right) L\Delta t\end{aligned} \tag{10}$$

Pursuit

In the pursuit phase, the lead aircraft attempts to drive the evader toward the capture area by positioning itself so that the evader's attempt to escape will lead him in the desired direction. The other aircraft climb to a position to prevent the complications of collision avoidance, and attempt to maintain observation of the target even if it leaves the pursuit aircraft's field of view.

Fig. 2: Aircraft transition to pursuit mode.

TEST AIRCRAFT AND EXPERIMENTAL CONDITIONS

GTMax

A Yamaha RMAX based research UAV, Figure 3, is utilized for the simulation and flight test activities under this effort. The system consists of four major elements: the basic Yamaha RMAX airframe, a modular avionics system, baseline software, and a set of simulation tools. Under nominal conditions, the flight controller can maintain an average tracking error of about 1 foot. The system also makes use of a Sick LD-MRS scanning laser range finder which has achieved ranges of 100 to 200 feet in practice. Further details of the configuration and performance of this system is explained in detail in (Ref. 20).

Fig. 3: GTMax autonomous rotary-wing research platform.

Georgia Tech UAV Simulation Tool

Simulation is performed using the Georgia Tech UAV Simulation Tool (GUST), a system which supports a broad range of simulations, from pure software-in-the-loop (SITL) running all processes on a single executeable, to hardware-in-the-loop (HITL) simulations exercising flight hardware through a simulation interface, to injecting simulated sensor data to the real aircraft in flight. The simulator models the system at a very granular level including, for example, binary serial data transmission between components (Ref. 21).

Experiment Description

The experiments were conducted with two goals; first, to identify qualitative aspects of the search and pursuit algorithm and problem. Second, speed of search and number of aircraft were varied to gauge their impact on the ability of the aircraft to search the area and drive the evader to the capture location. The simulations contain the greater range of independent variables, as the flight tests were conducted on a more limited basis due to time and risk constraints.

Two main categories of dependent variables were considered for analysis, evaluating each of the three elements of the search and pursuit algorithm. The measurements of the search area were collected to examine the amount of coverage varying with time. The estimates of the evader and his behavior parameter capture the performance of the evader estimator (though truth data for the evader in flight test is not known exactly). The estimated evader location was also used to evaluate the pursuit approach.

Each experiment was set at the Selby Combined Arms Collective Training Facility (CACTF), Fort Benning, Georgia (Figure 4). This is a small urban area with numerous buildings and roads. The simulated environment includes no wind or weather disturbances. Flight tests were all conducted in daylight with good conditions. Weather conditions in the area of the test site are summarized in Table 1.

The parameters of the search and pursuit algorithms which remained constant between experiments are listed in Table 2. For the simulation, the evader was given a maximum running

Fig. 4: Aerial View of Selby CACTF at Fort Benning, Georgia.

Table 1: Weather at Ft. Benning, GA (MFBGG1)

Parameter	
Mean Temperature (°F)	65
High Temperature (°F)	82
Mean Windspeed (ft/s)	2.9
Max Steady Windspeed (ft/s)	20.5
Max Gust Windspeed (ft/s)	24.9
Precipitation (in)	0.00

[a]Courtesy Weather Underground, www.wunderground.com

speed of 10 ft/s (roughly equivalent to a 30 seconds for a 100 m dash or 9 minutes for a mile). In each case, the evader's initial position was roughly at the center of the search area, and the designated capture area is the south end of the search area.

Table 2: Search and Pursuit Parameters

Parameter	
Search Area Long Dimension (ft)	1013
Search Area Narrow Dimension (ft)	383
Search Area Size (approx) (ft^2)	390,000
Search Area Map Resolution (ft)	10
Notional Sensing Range (ft)	500
Aircraft Separation (ft)	75
Mapping Acceleration (ft/s^2)	3
Pursuit Speed (ft/s)	15

For ease of comparison, the simulation experiments allowed the aircraft to search for about 120 seconds before revealing the evader, then pursue the evader for 120 seconds or until capture.

The evader was equipped with an Android smartphone, providing the aircraft with its position updates at approximately 1 Hz. The aircraft used an onboard database to determine line of sight to the phone. The evader was given general instructions of how to behave as detailed above, with the exception that random changes in escape direction should be very limited.

RESULTS AND DISCUSSION

Simulation

The results of the coverage phase of the search missions are shown in Figures 5 through 7. These results imply two conclusions; first, that more than one aircraft can more completely and uniformly search an area, though not drastically so. The second is that most of the search area is covered in the first 60 to 90 seconds of the mission, and reaches a relatively steady state of coverage when considering the staleness of a given observation.

In Figures 5 and 6, black signifies area outside the search zone, white as areas that haven't been searched yet or haven't been searched in so long that they are considered "stale". For the purposes of this work, any area that hasn't been searched in the last 120 seconds is considered stale. The remainder of the colors signify the recency of the map–hot colors are most recent, while the cool colors are nearly stale. The streaks of white in Figure 6 are an artifact of aircraft conflicting terrain data and these areas should be considered as solid color matching nearby colors.

A comparison of the single aircraft and two-aircraft scenarios confirm the intuitive result that more aircraft provide more coverage area, and overall more recent coverage.

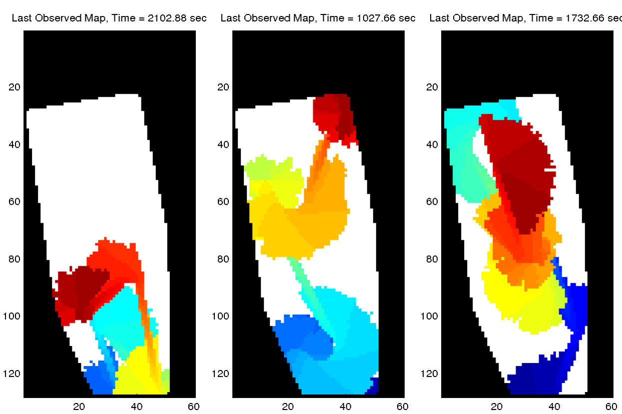

(a) 15 fps (b) 20 fps (c) 25 fps

Fig. 5: Comparison of coverage, single aircraft after 120 seconds of search.

Figure 7 provides an example of what the search paths of this algorithm look like, laid over the boundary of the search area. The circular shapes are indicative of the algorithm's ability to both ensure that directional sensors sweep in all directions and look at the buildings from many angles, eliminating possible hiding places.

The evader estimator did a fair job considering the simplicity of the filter. Because the measurements from the notional

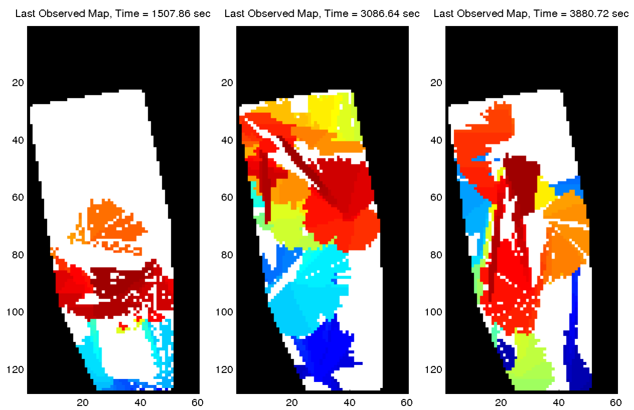

(a) 15 fps (b) 20 fps (c) 25 fps

Fig. 6: Comparison of coverage, two aircraft after 120 seconds of search.

sensor were positional with low noise, the estimate is quite accurate for the four kinematic states of the evader (Figures 8 through 11). The behavior estimator appears to be a good deal worse (Figure 12); however, in terms of its ability to adapt to the evader's changing behavior, it performed quite well, being able to ultimately drive the evader to the capture location (Figure 13).

Finally, an example of the pursuit is shown in Figure 13 by measuring the evader's distance from the capture area and examining how quickly the evader is progressing toward the capture location. Notably, the graph appears periodic—the evader can stave off being driven to the capture location by changing direction, but the filter adapts in time to make net progress toward the goal.

Flight Test

Because of limited resources and time, flight tests were conducted only for the multi-aircraft scenario, and flown at 10 ft/s to mitigate risk to the aircraft and to participants on the ground. Additionally, the search and pursuit phases were tested separately. The coverage map for this test is shown in Figure 14. The coverage maps are in general agreement with simulation. The later time in the search is used to offset the slow flight of the aircraft. Video stills of this flight are shown in Figures 15, 16, and 17.

Evader estimation was significantly more difficult in flight than in simulation largely due to the phone providing position updates at a low rate. Figures 18 and 19 show the performance of the estimator for the positional states. The action of the line-of-sight model can be seen in these figures, as the estimate drifts with no measurement around 240 seconds, 270 seconds, 350 seconds, 550 seconds, and finally at 590 seconds, each time quickly latching back on to the measurement once back in line of sight. However, the filter failed in estimation of velocity states and evasion direction. The aircraft was not able to drive the evader to the capture area using the pursuit logic in the time allotted.

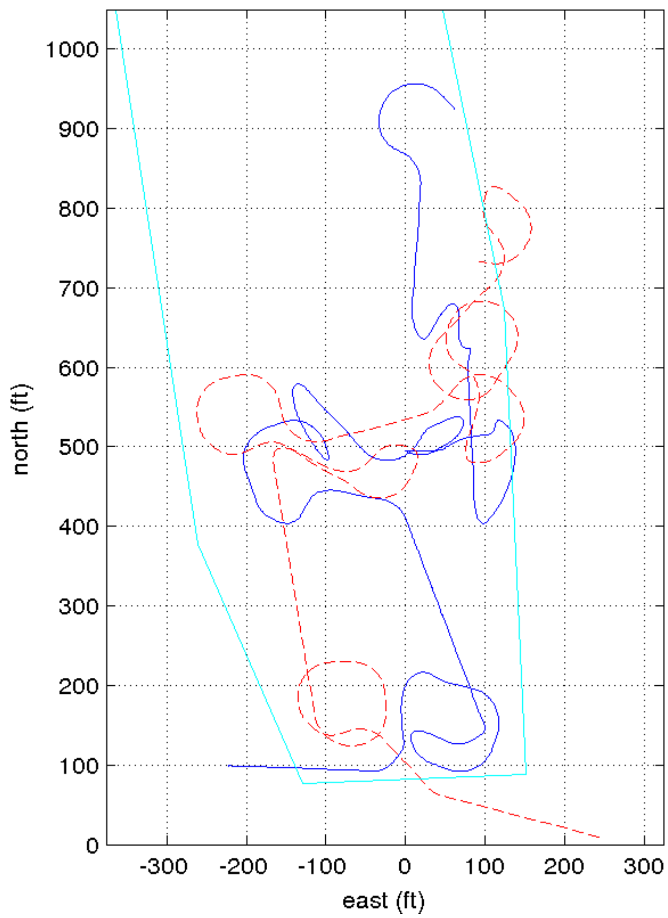

Fig. 7: Sample search pattern, two aircraft at 15 fps after 120 seconds. Search area boundary in cyan.

Discussion and Future Work

From the beginning of this effort, the basic philosophy was to develop the search and pursuit strategies with a simple, modular approach as a proof-of-concept. This was done for two reasons. First, multi-agent autonomy creates a complex environment where many systems on individual aircraft interact with each other and with the other agents (for example, collision avoidance, data sharing, terrain avoidance, and active task collaboration). The demands incremental development that is conducive to isolating problems. Second, past research has shown that simple individual behaviors can often give rise to more complex social behaviors (see (Refs. 1, 2)). The framework which could contain more complex algorithms has been developed and is ready to support further research goals. Considering the results presented here, our approach achieved our goals, while leaving plenty of room for deeper investigation.

Though the centralized nature of optimal coverage control presented in (Ref. 12) and related papers does not fit with the our desire to decentralize, a similar approach perhaps could be adapted to improve over the semi-random search technique used here. The coverage heat maps provide a useful visualization tool to evaluate the effectiveness of the search, but a single metric of search quality could be potentially more useful

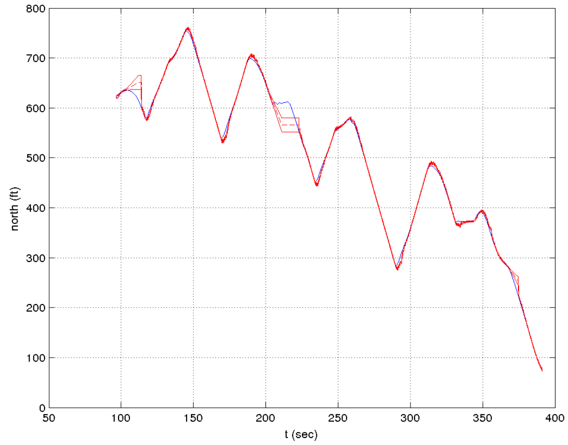

Fig. 8: North coordinate estimate with time. Truth (solid blue), estimate (dashed red), and 2 σ bounds (solid red) shown.

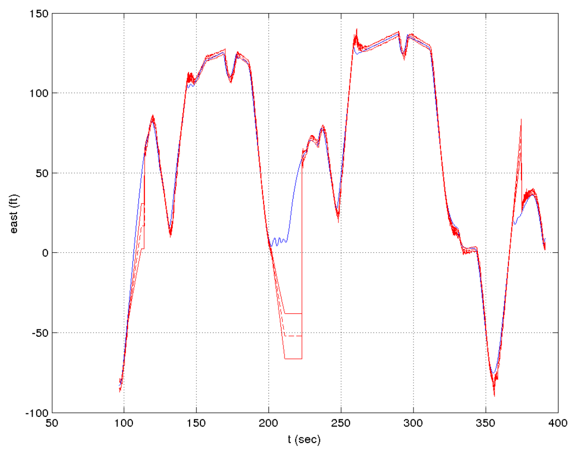

Fig. 9: East coordinate estimate with time. Truth (solid blue), estimate (dashed red), and 2 σ bounds (solid red) shown.

for analysis. These metrics ideally could be used to estimate confidence bounds on the likelihood of finding an evader in given period of time.

The estimators used to determine the state and behavior of the evader were not able to deal with the nonlinearities presented by the relatively dense urban environment. Similarly, the behavior of the evader was very oversimplified and does not represent what a real adversary may attempt to do. In future work, more sophisticated estimators, for example a particle filter, could be used to account for the complexities of urban terrain and unpredictable human behavior. A particle filter, in particular, would have the great advantage of being able to improve the estimate by incorporating the much more plentiful negative information about the evader's location, and providing a non-Gaussian probability distribution of his location. Using this information, the controller could select an optimal path by finding the path with maximum likelihood of

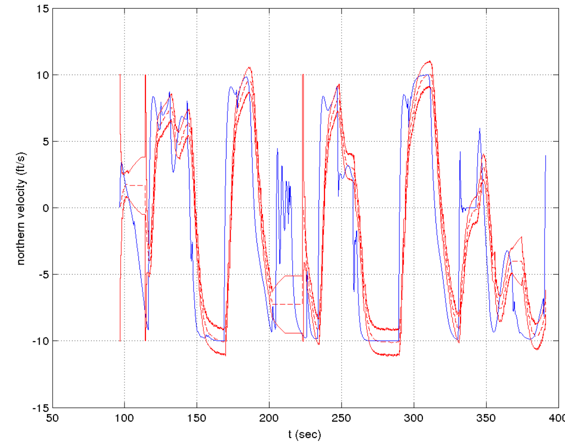

Fig. 10: Northern velocity estimate with time. Truth (solid blue), estimate (dashed red), and 2 σ bounds (solid red) shown.

detection. The evader's behavior model and the pursuit model would also benefit from a more sophisticated approach, using more abstract objectives (i.e. "don't be seen") rather than just maintaining a strictly kinematic rule set.

CONCLUSION

The efforts described in this paper include development of an approach to solve a scenario driven search-and-pursuit challenge problem, and simulation and flight test experiments studies to test the capabilities of this approach.

The framework to enable multi-aircraft interaction and collaboration has been further developed. Simulation results evaluated the ability of the algorithm to coordinate aircraft to search a selected area, find a target, estimate his behavior, and use knowledge of his behavior to drive him toward capture in a realistic urban environment. Flight test results examined the sub-parts of the approach independently, and generally validated the simulation results. Future work may investigate more sophisticated approaches to search, estimation, and pursuit in complex terrain.

ACKNOWLEDGMENTS

The authors would like to acknowledge the support and funding of the Sikorsky Aircraft Company. Additionally, would like to thank several contributors without whom this work would not be possible: Jeong Hur, Henrik Christopherson, Dmitry Bershadsky, Daniel Magree, and Kirk Simpson, as well as the staff of the Maneuver Battle Lab at Fort Benning, Georgia.

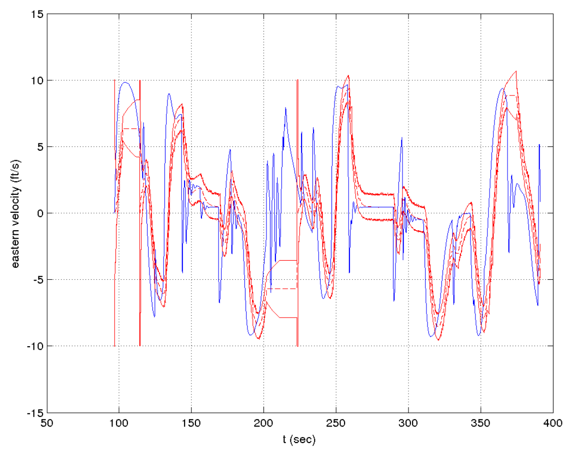

Fig. 11: Eastern velocity estimate with time. Truth (solid blue), estimate (dashed red), and 2 σ bounds (solid red) shown.

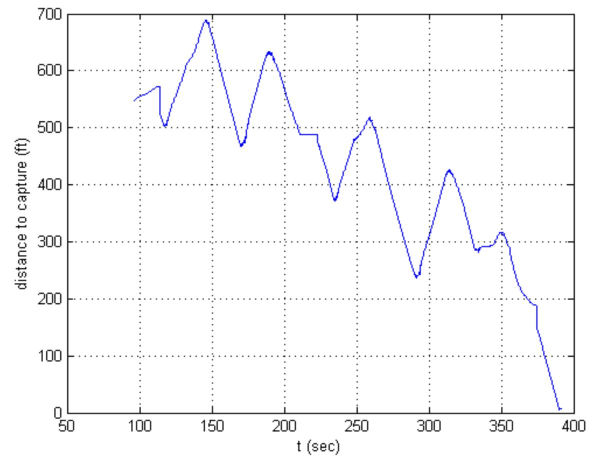

Fig. 13: Distance from capture as a function of time.

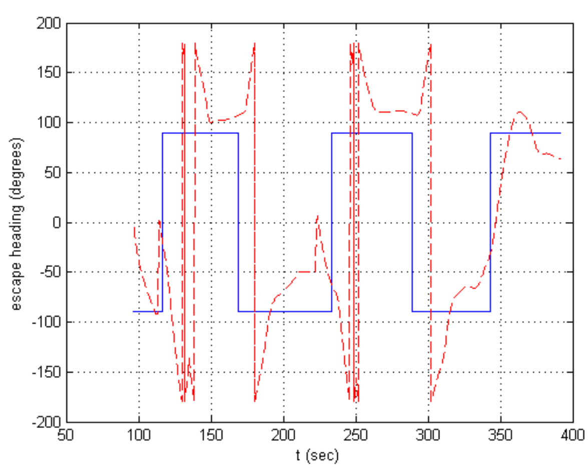

Fig. 12: Behavior estimate with time. Truth (solid blue) and estimate (dashed red) shown.

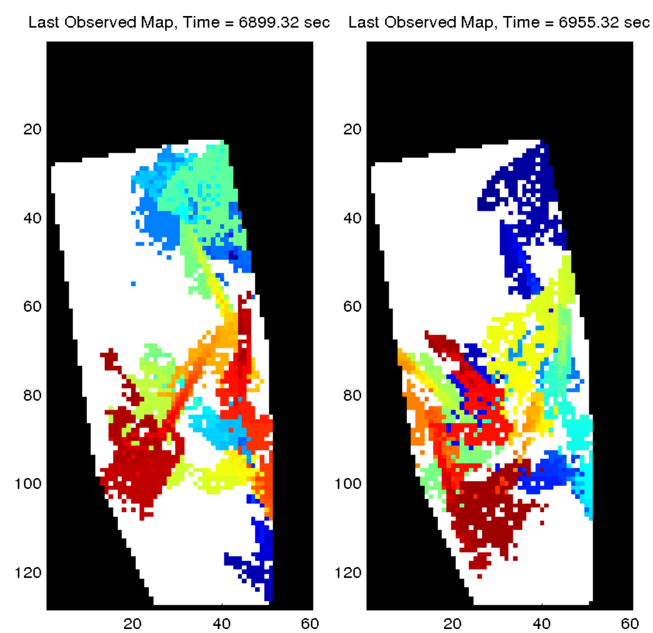

Fig. 14: Heat maps showing coverage of the search area approximately 120 seconds and 295 seconds into the mission.

Fig. 15: Two RMAX helicopters searching the area.

Fig. 16: Air-to-air footage from the nose of one RMAX of the other during the search phase of the mission.

Fig. 17: Ground station footage of the pursuit aircraft tracking the evader.

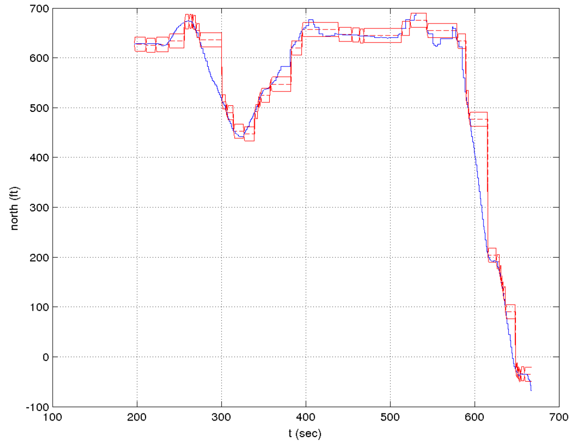

Fig. 18: North coordinate estimate with time. Phone reported position (solid blue), estimate (dashed red), and 2 σ bounds (solid red) shown.

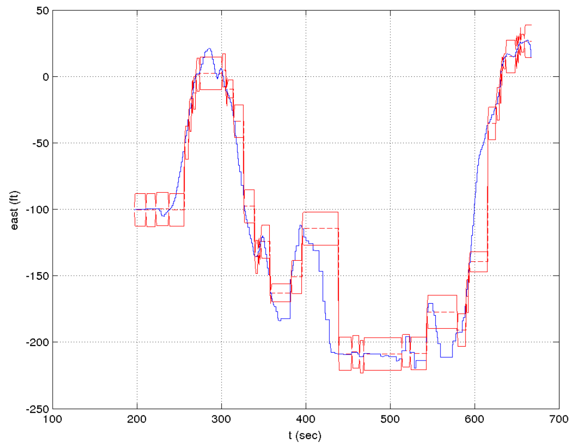

Fig. 19: East coordinate estimate with time. Phone reported position (solid blue), estimate (dashed red), and 2 σ bounds (solid red) shown.

REFERENCES

[1]Balch, T. and Arkin, R. C., "Behavior-based formation control for multirobot teams," *IEEE Transactions on Robotics and Automation*, 1998, pp. 1–15.

[2]Balch, T., "Social Potentials for Scalable Multi-Robot Formations," *International Conference on Robotics and Automation*, 2000.

[3]Parker, L. E., "Heterogeneous multi-robot cooperation," Technical report, MIT Artificial Intelligence Laboratory, 1994.

[4]Bruce, J. R. and Veloso, M., "Real-time randomized path planning for robot navigation," *Robots and Systems, 2002. IEEE/RSJ*, 2002.

[5]Luna, R. and Bekris, K. E., "Efficient and complete centralized multi-robot path planning," *2011 IEEE/RSJ International Conference on Intelligent Robots and Systems*, September 2011, pp. 3268–3275.
doi: 10.1109/IROS.2011.6095085

[6]Snoeyink, J., van den Berg, J., Lin, M., and Manocha, D., "Centralized Path Planning for Multiple Robots : Optimal Decoupling into Sequential Plans," Robotics: Science and Systems, 2009.

[7]Godbole, D. N., "Control and coordination in uninhabited combat air vehicles," Paper June, Proceedings of the Control Conference, 1999. . . . , 1999.

[8]Ribichini, G. and Frazzoli, E., "Efficient Coordination of Multiple-Aircraft Systems," Paper December, IEEE Conference on Decision and Control, 2003.

[9]Anderson, B. D. O., Fidan, B., Yu, C., and van der Walle, D., "UAV Formation Control : Theory and Application," *Recent Advances in Learning and Control*, Springer, 2008, pp. 1–20.

[10]Macwan, A., Nejat, G., and Benhabib, B., "Optimal Deployment of Robotic Teams for Autonomous Wilderness Search and Rescue," 2011 IEEE/RSJ International Conference on Intelligent Robots and Systems, 2011.

[11]Yoon, S. and Qiao, C., "A New Search Algorithm using Autonomous and Cooperative Multiple Sensor Nodes," IEEE INFOCOM 2007 - 26th IEEE International Conference on Computer Communications, 2007.
doi: 10.1109/INFCOM.2007.114

[12]Mathew, G. and Mezic, I., "Spectral Multiscale Coverage: A uniform coverage algorithm for mobile sensor networks," *Proceedings of the 48h IEEE Conference on Decision and Control (CDC) held jointly with 2009 28th Chinese Control Conference*, December 2009, pp. 7872–7877.
doi: 10.1109/CDC.2009.5400401

[13]Mathew, G., Surana, A., and Mezi, I., "Uniform Coverage Control of Mobile Sensor Networks for Dynamic Target Detection," IEEE Conference on Decision and Control, 2010.

[14]Mathew, G. and Mezić, I., "Metrics for ergodicity and design of ergodic dynamics for multi-agent systems," *Physica D: Nonlinear Phenomena*, Vol. 240, (4-5), February 2011, pp. 432–442.
doi: 10.1016/j.physd.2010.10.010

[15]Hubenko, A., Fonoberov, V. a., Mathew, G., and Mezić, I., "Multiscale Adaptive Search." *IEEE transactions on systems, man, and cybernetics. Part B, Cybernetics : a publication of the IEEE Systems, Man, and Cybernetics Society*, Vol. 41, (4), February 2011, pp. 1076–1087.
doi: 10.1109/TSMCB.2011.2106207

[16]Surana, A., Mathew, G., and Kannan, S., "Coverage Control of Mobile Sensors for Adaptive Search of Unknown Number of Targets," International Conference on Robotics and Automation, 2012.

[17]Mathew, G., Kannan, S., Surana, A., Bajekal, S., and Chevva, K. R., "Experimental Implementation of Spectral Multiscale Coverage and Search Algorithms for Autonomous UAVs," *AIAA Guidance, Navigation, and Control (GNC) Conference*, August 2013, pp. 1–13.
doi: 10.2514/6.2013-5182

[18]Johnson, E. N., Mooney, J. G., Magree, D. P., White, M., Hartman, J., and Sahasrabudhe, V., "Collaborative Mapping and Search for Autonomous Helicopters," AHS Annual Forum, 2013.

[19]Johnson, E. N., Mooney, J. G., White, M., Hartman, J., and Sahasrabudhe, V., "Terrain Height Evidence Sharing for Collaborative Autonomous Rotorcraft Operation," AHS International Specialists' Meeting on Unmanned Rotorcraft and Network Centric Operations, 2013.

[20]Johnson, E. N. and Schrage, D. P., "System Integration and Operation of a Research Unmanned Aerial Vehicle," *AIAA Journal of Aerospace Computing, Information, and Communication*, Vol. 1, (1), January 2004, pp. 5–18.
doi: 10.2514/1.4424

[21]Johnson, E. N. and Mishra, S., "Flight Simulation for the Development of an Experimental UAV," AIAA Modeling and Simulation Technologies Conference, 2002.